

# Research on 3-D Surface Crack Growth in Rock-like Material under Uniaxial Tension

Lei Yang<sup>1\*</sup>, Yujing Jiang<sup>2</sup>, Shucui Li<sup>3</sup>, Bo Li<sup>2</sup> and Tanabashi Yoshihiko<sup>2</sup>

<sup>1</sup>Graduate School of Science and Technology, Nagasaki University, Nagasaki 852-8521, Japan

<sup>2</sup>Faculty of Engineering, Nagasaki University, Nagasaki 852-8521, Japan

<sup>3</sup>Research Center of Geotechnical and Structural Engineering, Shandong University, Jinan 250061, China

\*E-mail: sdylei@gmail.com

At present, the mechanism of crack growth in rock masses remains one of the most fundamental and promising problems in academic and engineering aspects. In this study, uniaxial tension experiments were carried out to investigate the propagation processes of 3-D surface crack in artificial rock-like samples, and the influence of crack dip angle on material strength and crack growth pattern. Experimental results indicate that the load-deformation processes of samples containing surface crack exhibit 4-stage behaviors. The crack dip angle has obvious effect on sample strength. Tensile wing crack and lateral growth are the main propagation patterns of surface crack. Near the sample surface, surface crack grows similar to 2-D mode. And in the interior of sample, crack grows in a 3-D mode.

**Key Words :** *Uniaxial tension, 3-D surface crack, propagation pattern, sample strength, wing crack.*

## 1. Introduction

Fractures like joints and cracks universally exist in rock masses, playing an important role in the strength and failure behaviors of rock masses. With the increase of external loads, pre-existing cracks in rock masses will initiate, grow and join with other neighbouring ones<sup>1)</sup>. The propagation and coalescence of cracks change the distribution of stress field in rock masses, and cause local stress concentration which leads to the failure of rock masses<sup>2)</sup>. Failure of a rock mass is always preceded by processes of initiation and accumulation of new cracks and growth of existing ones<sup>3)</sup>. Therefore, the existence of cracks in rock masses is a potential threat to the safety of rock structures, such as tunnel and dam. At present, the mechanism of crack growth and coalescence in rock masses remains one of the most fundamental and promising problems in both academic and engineering aspects.

To avoid the difficulties in the processes of phenomenon observation and result analysis, a number of experimental and theoretical studies have been performed by modeling the natural cracks as 2-D ones (plate with through cracks) to investigate the crack propagation and coalescence mechanisms under compression<sup>4), 5)</sup>. However, most pre-existing cracks in nature are three-dimensional, either fully embedding in rock masses (defined as 3-D internal cracks) or semi-embedding in rock masses (defined as 3-D surface cracks). The simplification of 3-D cracks into 2-D model can bring

convenience to analysis, but would lose lots of 3-D geometrical and mechanical characteristics and result in great deviation from the actual situations. In recent years, the research on the growth mechanisms of 3-D cracks attracts more and more attention.

Adams and Sines performed experiments to investigate the propagation pattern of 3-D elliptical crack in PMMA material under compression, and they observed the initiation and propagation processes of squamous cracks<sup>6)</sup>. Through compression tests, Dyskin et al investigated the growth rules of 3-D internal crack in various materials, including transparent casting resin, cement, and mortar, taking into account the influence of shape and location of cracks on their growth<sup>7)</sup>, and proposed a 3-D model of wing crack propagation and interaction<sup>8)</sup>. To observe the growth process of internal crack, Li et al conducted uniaxial compression tests on brittle ceramic samples using a real-time CT scanning apparatus. They obtained some important parameters such as the sample strength and the length of wing crack<sup>9)</sup>. Wong et al investigated the growth processes of 3-D surface crack in PMMA material under compression. They also proposed the propagation pattern of anti-wing cracks from pre-existing surface crack in gabbro samples, and analyzed the growth conditions of surface crack, including the initiating location and propagation direction<sup>10)</sup>.

Most previous studies were carried out under various compressive conditions. At present, there have been rare researches on the growth mechanisms of 3-D crack in rock masses under tensile conditions,

especially the influence of crack propagation on sample mechanical properties, due to the fact that in most cases rock masses encountered in rock engineering seem to be only subjected to compression loads. However, the tensile stress exists widely in almost all rock masses, and due to the low tensile capacity of rock, the failure of rock masses usually correlates with the tensile stress.

In this study, uniaxial tension experiments were carried out to investigate the propagation processes of 3-D surface crack in artificial rock-like samples, and the influence of crack dip angle on material strength and crack growth pattern.

## 2. Experimental techniques

### (1) Experimental material

Utilization of natural rock samples could truthfully represent the mechanical behaviors of rock. However, the complexity of rock internal structure brings difficulties to the analyses of test results, while the use of natural rock will face the difficulty of sample manufacture. As an alternative, some transparent rock-like materials, such as casting resin and PMMA, could help observe the crack growth process. However, some of mechanical properties like the brittleness and heterogeneity are different from those of rock. Therefore, an ideal rock-like material needs not only to have the same physical and mechanical properties with rock, but also to be convenient to manufacture samples and to create pre-existing 3-D cracks.

In this study, a new rock-like mortar material (mixture of Portland cement, water and river sand) was developed to simulate sandstone usually encountered in engineering practices. The compressive strength of cement was 32.5 MPa. The sand was to ensure the heterogeneity of mortar. The mixing ratio of raw materials by weight was cement: sand: water= 1: 2.34: 0.35. In addition, three kinds of additives (early strength agent, water reducing agent and waterproofing agent) were added to ensure high strength and good workability of the mortar material. Tests on physical and mechanical parameters of mortar material were conducted. As listed in Table 1, the rock-like material exhibits close properties with typical sandstone (see Ref. 4), with good brittleness due to the high ratio of compressive to tensile strength.

### (2) Sample preparation

The sketch of the shape and size of sample with pre-existing crack is shown in Fig-1a. The sample has a bone-like shape, which helps reduce stress concentration when applying tensile stresses on the upper and lower boundaries. The sizes of sample are:  $W_0 \times H_0 \times T_0 = 100 \text{ mm} \times 200 \text{ mm} \times 50 \text{ mm}$ ,  $H_1 = H_2 = 50 \text{ mm}$ ,  $W \times H \times T = 50 \text{ mm} \times 100 \text{ mm} \times 50 \text{ mm}$ . A piece of polyester film with the thickness of 0.25 mm was embedded into the center of sample to simulate

Table 1 Physical and mechanical parameters of mortar and sandstone

Physico-mechanical properties	Index	Unit	Mortar	Sandstone
Density	$\rho$	$\text{g/cm}^3$	2.3	1.2~3.0
Compressive strength	$\sigma_c$	MPa	35.5	20~170
Tensile strength	$\sigma_t$	MPa	2.8	2~25
Modulus of elasticity	$E$	GPa	17.9	3.0~35.0
Poisson's ratio	$\nu$	-	0.19	0.1~0.3
Fracture toughness	$K_{IC}$	$\text{MPa}\cdot\text{m}^{0.5}$	0.51	0.22~2.26

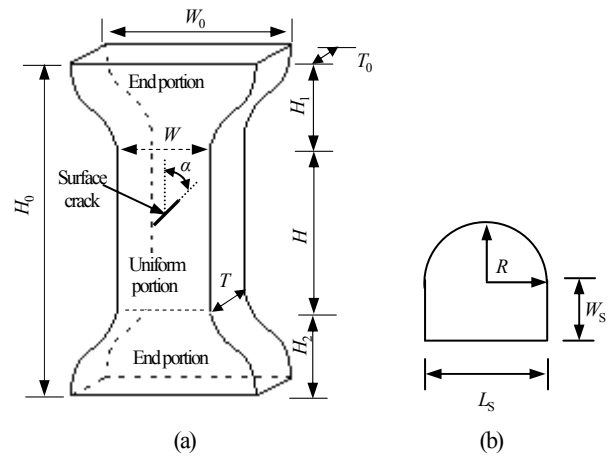


Fig-1 Shape and size of samples and pre-existing surface crack. (a): Sample; (b): Pre-existing surface crack (top view)

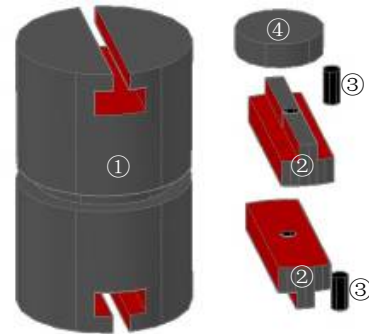


Fig-2 The location apparatus for bonding tension experiments on rock-like material. ①: Cylindrical pile; ②: Sliding block; ③: Bolt; ④: Cushion block

surface crack with the size of  $L_s = 20 \text{ mm}$ ,  $W_s = 10 \text{ mm}$  and  $R = 10 \text{ mm}$  (Fig-1b). The contour of pre-existing surface crack consists of straight parts and arc part, corresponding to the stress conditions near the sample surface (plane stress condition) and in the sample interior (3-D stress condition) respectively, to investigate the different crack

propagation patterns.

In order to study the influence of crack dip angle on the sample strength and crack propagation pattern, 5 samples each containing a single surface crack with different dip angle were processed. The dip angle of surface crack  $\alpha$  ranges from  $30^\circ$  to  $90^\circ$ , with an increment of  $15^\circ$ .

The sample preparation process can be divided into 4 steps. Firstly, mix the raw materials of mortar with a stirring machine, until the mixture exhibits good uniformity and workability. Secondly, assemble the sample mold, within which the polyester film was held by cotton threads at specified location and dip angle. Then fill the mold with the material mixture, and vibrate it with a vibrating machine for 180 seconds. Finally, put the sample into a curing box for 7 days, with proper temperature and humidity conditions. After those steps, the sample can be used for experiments.

### (3) Experimental apparatuses

Samples were uniaxially loaded by means of a 3000 kN servo-control rigid digital testing machine in a displacement controlled loading mode at a loading rate of 0.002 mm/s. Measuring ranges of load and displacement sensors are 100 kN and  $\pm 5$  mm respectively. The stress and strain data were collected by a data acquisition system of the testing machine.

A location apparatus for bonding load cells on rock-like materials was designed and processed, as shown in Fig-2. The location apparatus consists of a cylindrical pile and two sliding blocks. Samples were bonded with the upper and lower steel cushion blocks connecting to the load cell and location apparatus, by using a structure adhesive with a tensile strength of 18 MPa, as shown in Fig-3. The location apparatus can not only slide along the lower and upper sliding blocks but also can rotate freely along the axis of the cylindrical pile. This apparatus is effective to ensure the axial tension. It should be noticed that all the parts of experimental device were made of steel with high strength and stiffness to reduce the interference to the axial displacement.

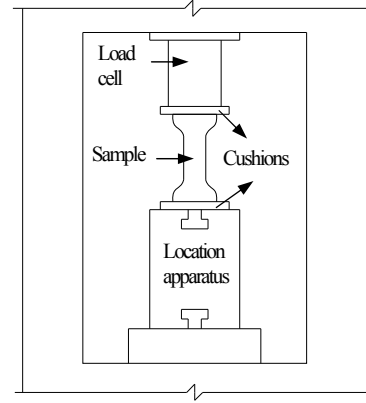


Fig-3 Experimental apparatus and its application

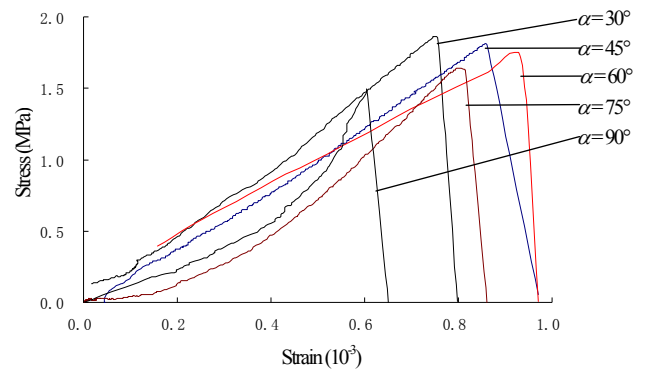


Fig-4 Uniaxial tensile stress-strain curves of samples containing single surface cracks

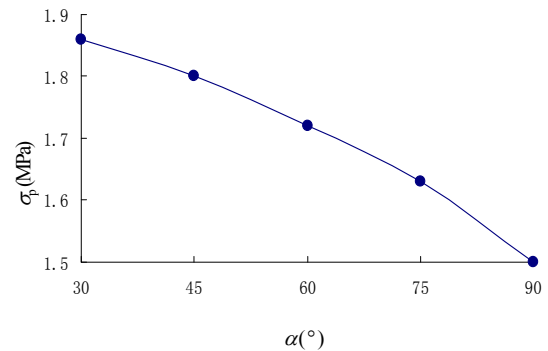


Fig-5 Influence of surface crack dip angle on sample strength

## 3. Experimental results

### (1) Mechanical behaviors of samples

Uniaxial tension experiments were performed on samples containing single surface cracks with varying crack dip angles. The stress-strain curves of different samples were obtained, as shown in Fig-4. Here, the stress stands for the average stress in the uniform-cross segment, being obtained by  $F/A_0$ , where  $F$  is the external loads and  $A_0$  is the area of cross section in the uniform-cross segment. The strain represents the average strain of the sample, being obtained by  $D/H_0$ , where  $D$  is the total deformation of sample and  $H_0$  is the height

of sample.

Those curves indicate that despite of the difference in crack dip angle, the curve shapes and the load-deformation processes of all samples are similar except for the tensile strengths.

The load-deformation processes of samples containing pre-existing surface cracks under uniaxial tension can be divided into four stages, including flaws opening stage, elastic deformation stage, elastic and plastic deformation stage and failure stage. In the flaws opening stage, the pre-existing crack and micro flaws in samples open gradually with the increase of tensile stresses, resulting in the nonlinearity in the initial parts of curves. After that, the samples

exhibit elasticity, producing a linear portion on the stress-strain curve. During the elastic and plastic stage, both elastic and plastic deformations are produced due to the increased tensile stress. This stage is much shorter than the previous elastic stage, and little plastic deformations would lead to the overall failure of samples. In the failure stage, the samples fracture abruptly with the quick drop of curves after the tensile stresses reach their peaks.

The change of dip angle of pre-existing surface crack has obvious effect on sample strength. Fig-5 shows the relationship between crack dip angles  $-\alpha$  and sample strengths  $-\sigma_p$ , demonstrating that the sample strength decreases with the increase of crack dip angle. This fact can be explained that the component of tensile stress which is perpendicular to the initial crack plane increases as the crack dip angle increases. The normal component of tensile stress can lead to the mode I fracture easily.

Through Fig-4, it also can be found that when the crack dip angle is large, e. g.  $\alpha=75^\circ$  and  $90^\circ$ , the stress-strain curve presents obvious nonlinearity. In the cases of large crack dip angles, the fracture happens easily, and the propagation of crack produces more plastic deformation of sample relatively, leading to the nonlinearity.

## (2) Fracture states of samples

The fracture process of sample containing surface crack was observed during the uniaxial tensile test, and the failure states of samples are shown in Fig-6, Fig-7 and Fig-8 ( $\alpha=30^\circ$ ,  $60^\circ$  and  $90^\circ$ , respectively). Experimental results indicate that the overall fracture initiates from the pre-existing surface crack, with the fracture trace and section locating in the middle of sample (in the uniform-cross segment, Fig-6a, Fig-7a and Fig-8a). At the beginning, macro wing cracks initiate from the tips of initial crack on the front surface of sample. With the increase of tensile stress, the wing cracks grow quickly in the direction perpendicular to the tensile stress. Then macro cracks were observed on the lateral surfaces of sample, which grew from the front surface to back surface of sample. At last, the fracture happened on the back surface, and the sample broke into two parts.

It can be derived from the experimental phenomena that the fracture mode and crack growth process on the front surface of sample are similar to those of 2-D crack (the penetrating crack, Fig-6b, Fig-7b and Fig-8b). However, on the back surface of sample, the fracture trace is quite different, which is at a smaller angle to the horizontal direction than the initial inclination of surface crack (Fig-6c, Fig-7c and Fig-8c), as listed in Table-2. It also can be found that the dip angle of surface crack has effect on the fracture trace inclination on the back surface of sample. The fracture trace inclination increases with the increase of crack dip angle.

Through observing the fracture sections of failure samples, it indicates that the wing crack and lateral growth are the main fracture patterns of samples under tension (Fig-6d, Fig-7d and Fig-8d). The

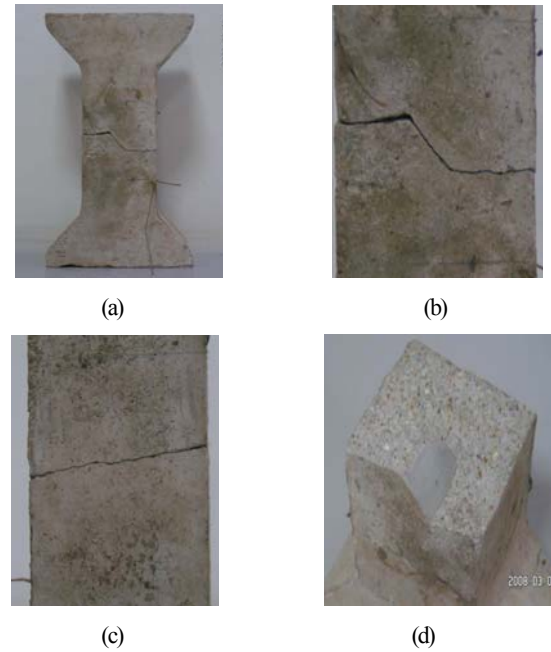


Fig-6 Failure states of sample with  $\alpha=30^\circ$ . (a): Fractured sample; (b): Fracture trace on front surface; (c): Fracture trace on back surface; (d): Fracture section

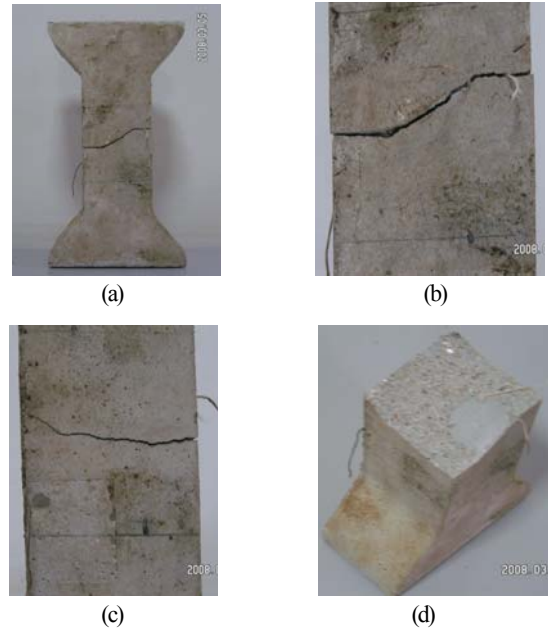


Fig-7 Failure states of sample with  $\alpha=60^\circ$ . (a): Fractured sample; (b): Fracture trace on front surface; (c): Fracture trace on back surface; (d): Fracture section

propagation of pre-existing surface crack forms a spatial distortion plane, which leads to the overall fracture. The propagation pattern of surface crack in the interior of sample exhibits typical 3-D characteristics, such as the wrapping wing crack and the spatial distortion plane. Due to the constraint of 3-D stress, the propagation plane of initial crack is distorted. Therefore, the fracture trace on the back surface is different from that on the front surface. Internal 3-D

stresses affect not only the growth trace of crack, but also the mechanical behaviors of sample.

In a range of thickness which is small enough from the front surface of sample, that portion of sample with surface crack can be regarded as under plane stress condition. However, the crack embedded in the sample interior is under 3-D stress conditions. In addition, the stress concentration exists in the portion where the surface crack intersects with the front surface of sample. Therefore, the pre-existing crack grows more quickly on the sample surface than in the sample interior.

### (3) Propagation process of 3-D surface crack

From the experimental phenomena, the propagation process of surface crack in rock-like sample under uniaxial tension can be concluded. The propagation patterns of single surface crack can be divided into two categories, including the inclined crack pattern ( $0^\circ < \alpha < 90^\circ$ ) and the horizontal crack pattern ( $\alpha = 90^\circ$ ). The growth process of inclined surface crack is sketched in Fig-9. At the beginning of tension tests, the pre-existing surface crack and micro closed flaws in samples open gradually due to the tensile stress. However, the pre-existing surface crack do not propagate (Fig-9a). As the external stress increases, the wrapping wing cracks initiate from the front of initial crack (the straight parts and most of the arc part of surface crack contour), and the lateral growth initiates near the vertex of circular arc (Fig-9b). The lateral growth propagates in the initial crack plane all the time during the tests. The wing crack grows perpendicular to initial crack plane in the beginning, and then its growth direction changes to horizontal with the increase of tensile stress (Fig-9c). Finally, a spatial distortion plane formed by the combined propagation of wing cracks and lateral growth results in the overall fracture of sample (Fig-9d).

Near the sample surface, pre-existing crack grows like the 2-D mode. However, in the interior of sample, crack grows in a typical 3-D mode. Specially, the surface grows more quickly near the sample surface than in the interior of sample due to the free surface effect.

In the case of horizontal surface crack, only mode I fracture happens, and both the wing crack and lateral growth propagate in the initial crack plane, resulting in that the failure section is flat and perpendicular to the sample axis.

## 4. Conclusion

The propagation and coalescence of pre-existing cracks are important factors in the failure behaviors of rock masses. The growth mechanism of 3-D crack in rock masses remains one of the most fundamental and promising problems. However, there have been rare researches on crack growth under tensile condition. In this paper,

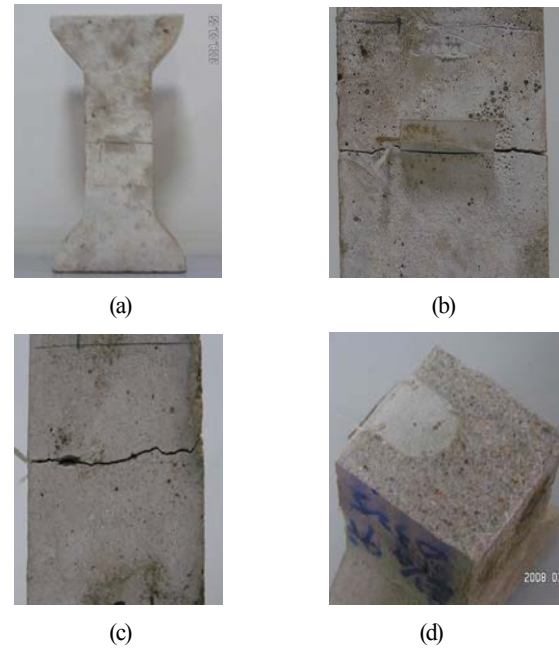


Fig-8 Failure states of sample with  $\alpha=90^\circ$ . (a): Fractured sample; (b): Fracture trace on front surface; (c): Fracture trace on back surface; (d): Fracture section

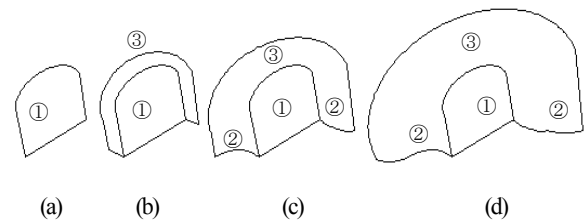


Fig-9 Propagation process of single inclined surface crack under tension. ①: Pre-existing surface crack; ②: Wing crack; ③: Lateral growth

Table-2 Relationship between the surface crack dip angle and the fracture trace inclination on the back surface of sample

Crack dip angle	30°	45°	60°	75°	90°
Fracture trace inclination	69°	76°	80°	81°	90°

uniaxial tension experiments have been performed on rock-like artificial samples to investigate the propagation process of 3-D surface crack and its influence on sample strength.

Experimental results indicate that the load-deformation processes of rock-like samples containing single surface cracks under tension exhibit 4-stage behaviors, including the flaws opening stage, the elastic deformation stage, the elastic-plastic deformation stage and the failure stage. The change of dip angle of pre-existing surface crack has obvious effect on sample strength, which decreases with the increase of crack dip angle.

The overall fracture initiates from the pre-existing crack, with the



fracture trace and section locating in the middle of sample. The fracture mode and crack growth process on the front surface of sample are similar to those of 2-D crack, while the growth pattern of pre-existing crack in the interior of sample exhibits typical 3-D characteristics. Tests indicate that the dip angle of surface crack has effect on the fracture trace inclination on the back surface of sample.

The wing crack and lateral growth are the main propagation patterns of 3-D surface crack under tension. A spatial distortion plane resulting from the combined propagation of wing crack and lateral growth can lead to the overall fracture of sample.

At present, the growth mechanisms of 3-D crack in rock masses under various stress conditions are still not well understood, due to the difficulty of quantitative stress evaluation in the interior of rock masses. In the future, some numerical researches will be performed to investigate the distribution of stress field and the stress concentration effects resulted from the cracks in rock masses.

#### References

- 1) Wong, R.H.C., et al. : Crack propagation from 3-D surface fractures in PMMA and marble specimens under uniaxial compression. *Int. J. Rock Mech. & Min. Sci.* 41(3), 1A07, 2004.
- 2) Bobet, A. : The initiation of secondary cracks in compression. *Engineering Fracture Mechanics*. 66, pp. 187-219, 2000.
- 3) Peng, S. and Johnson, A.M. : Crack growth and faulting in cylindrical specimens of Chelmsford granite. *Int. J. Rock Mech. & Min. Sci. & Geomech. Abstr.* 9, pp. 37-86, 1972.
- 4) Wong, R.H.C. and Chau, K.T. : Crack coalescence in a rock-like material containing two cracks. *Int. J. Rock Mech. & Min. Sci.* 35(2): pp. 147-164, 1998.
- 5) Bobet, A. and Einstein, H.H. : Fracture coalescence in rock-type materials under uniaxial and biaxial compression. *Int. J. Rock Mech. & Min. Sci.* 35(7), pp. 863-888, 1998.
- 6) Adams, M. and Sines, G. : Crack extension from flaws in a brittle material subjected to compression. *Tectonophysics*. 49, pp. 97-118, 1978.
- 7) Dysikin, A.V., et al. : Influence of shape and locations of initial 3-D cracks on their growth in uniaxial compression. *Engineering Fracture Mechanics*. 70, pp. 2115-2136, 2003.
- 8) Dysikin, A.V., Germanovich, L.N. and Ustinov, K.B. : A 3-D model of wing crack growth and interaction. *Engineering Fracture Mechanics*. 63, pp. 81-110, 1999.
- 9) Li, S.C., et al. : CT real-time scanning tests on rock specimens with artificial initial crack under uniaxial conditions. *Chinese Journal of Rock Mechanics and Engineering*. 26(3), pp. 484-492, 2007.
- 10) Guo, Y.S., et al. : Study on fracture pattern of open surface-flaw in Gabbro. *Chinese Journal of Rock Mechanics and Engineering*. 26(3), pp. 525-531, 2007.